

## **Title: Acyl phosphates as chemically fueled building blocks for self-sustaining protocells**

**Authors:** Oleksii Zozulia,<sup>1</sup> Christine M. E. Kriebisch,<sup>1</sup> Brigitte A. K. Kriebisch,<sup>1</sup> Héctor Soria Carrera,<sup>1</sup> Kingu Rici Ryadi,<sup>1</sup> Juliana Steck,<sup>1</sup> and Job Boekhoven<sup>1</sup>

### **Affiliations:**

<sup>1</sup> Department of Bioscience, School of Natural Sciences, Technical University of Munich, Lichtenbergstrasse 4, 85748 Garching, Germany.

### **Abstract**

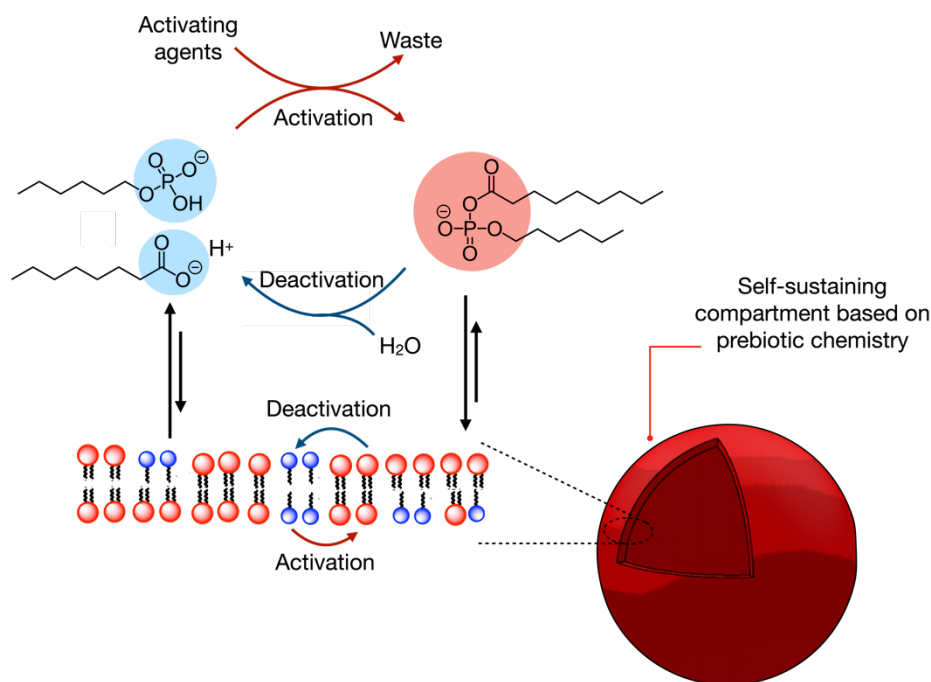
Lipids can spontaneously assemble into vesicle-forming membranes. Such vesicles serve as compartments for even the simplest living systems. Vesicles have been extensively studied for constructing synthetic cells or as models for protocells—the cells hypothesized to have existed before life. These compartments exist almost always close to equilibrium. Life, however, exists out of equilibrium. In this work, we studied vesicle-based compartments regulated by a non-equilibrium chemical reaction network that converts activating agents. Specifically, we use activating agents to condense carboxylates and phosphate esters into acylphosphate-based lipids that form vesicles. These vesicles can only be sustained when condensing agents are present, and without them, they decay. We demonstrate that the chemical reaction network can operate on prebiotic activating agents, opening the door to prebiotically plausible, self-sustainable protocells that compete for resources. In future work, such protocells should be endowed with a genotype, for example, based on self-replicating RNA structures that affect the protocell behavior to enable Darwinian evolution in a prebiotically plausible chemical system.

### **Introduction**

Compartmentalization is critical for extant life as it allows for the protection of biochemical reaction networks, prevents dilution, and prevents the invasion of parasites. In even the simplest forms of life, compartmentalization is achieved through phospholipids that spontaneously assemble into vesicles. Phospholipid-based vesicles have been studied extensively as a model for the cell wall or as the building blocks for synthetic cells.<sup>1-2</sup> Moreover, lipids are used as a protocell model for how life could have originated in a so-called “compartment-first hypothesis”.<sup>3-4</sup> Excitingly, even simple, prebiotically relevant lipids like fatty acids also spontaneously assemble into vesicles. Moreover, such vesicles can grow and spontaneously divide when supplied with building blocks.<sup>5-8</sup> While fatty acids can assemble into compartments and show exciting life-like behavior, there is a critical difference between such systems and life as we know it. Life maintains itself outside of equilibrium by

converting chemical energy and light into the building blocks. Even in homeostasis, a cell sustains itself by using resources to regulate its internal chemical reaction networks. Thus, in an approach towards the *de novo* synthesis of life but also to create models for compartments at the origin of life, self-sustainment outside of equilibrium should be considered. Therefore, we and others coupled the formation of compartments to non-equilibrium chemical reaction cycles.<sup>9-11</sup> In such a reaction cycle, a molecule with high chemical potential (that we refer to as fuel) is converted into a molecule with low chemical potential (waste).<sup>12-14</sup> Reaction cycles that convert methylating agents,<sup>15-16</sup> condensing agents,<sup>17-22</sup> acylating agents,<sup>23</sup> phosphorylating agents,<sup>24-25</sup> and reducing or oxidizing agents<sup>26-28</sup> have been well-explored. The fuel conversion transiently activates a molecule to assemble or phase-separate into a compartment. The activated state is shortlived and spontaneously reverts to its original non-activated state. Thus, at the expense of fuel, molecules are transiently activated to form dynamic, non-equilibrium compartments. The resulting compartments can, therefore, only nucleate when chemical energy is available. These compartments can grow or even divide when energy is abundant.<sup>29</sup> Finally, when all energy is consumed, the compartments decay into their original building blocks. Such self-sustaining compartments thus constantly compete for resources, making them an attractive model for protocells—protocells that do not produce new building blocks faster than their deactivation will naturally succumb, rendering their building blocks available for the competition. We envision that small advantages to individual protocells could be encoded in the protocell's pre-genotype, like self-replicating molecules like RNA within the protocells that aid the growth or even division of the protocells. In a scenario where energy is scarce or only periodically fed to the protocells, those with a genotype that favors growth could outcompete ones without. While some self-sustaining compartments have been described with exciting behavior like growth<sup>30</sup> and even division,<sup>31</sup> the number of examples that form vesicle-based compartments remains limited.<sup>24</sup> Moreover, examples that produce self-sustaining compartments based on prebiotically plausible chemistry are scarce.<sup>32</sup>

In this work, we developed a self-sustaining chemical system that produces non-equilibrium, transient vesicles based on simple, prebiotically plausible building blocks (Scheme 1). Specifically, we used fatty acids combined with alkyl phosphates as building blocks. When supplied with carbodiimides or prebiotically plausible activating agents, a reaction cycle starts to operate that produces acyl phosphates as an activated product. That product is labile and hydrolyzed to its precursor. The activated state, in its short lifetime, can assemble to form dynamic vesicles.



**Scheme 1.** The chemical reaction cycle based on acyl phosphate chemistry leads to the formation of transient lipids that form out-of-equilibrium compartments.

## Results and discussion

For the molecular design of the chemical reaction cycle, we studied various carboxylates, alkyl phosphate, and activating agents. As carboxylates, we explored hexanoic ( $C_6$ ) and octanoic acid ( $C_8$ ). For the alkyl phosphates, we synthesized hexyl ( $C_6P$ ) and octyl ( $C_8P$ ) phosphates as their disodium salts. The molecular design strategy was to form their corresponding acyl phosphate—a double-tailed molecule with an anionic phosphate head group. All of these starting components in the reaction cycle are well soluble in the 100 mM range in pyridine-containing MES-buffered water (200 mM), provided the pH remains above pH 6. Pyridine was added because of its ability to suppress the formation of N-acyl urea and to aid acyl phosphate formation.<sup>33-34</sup> We performed all experiments at 37 °C and under constant stirring.

Adding 20 mM EDC to a mixture of 40 mM  $C_6P$  and 40 mM  $C_8$  initiated the reaction network (Figure 1A). We investigated the kinetic profile of the reaction using HPLC and the LCMS (Figure 1B and Supplementary Figure S1-3). We observed that the 20 mM EDC was consumed within the first hour after its addition, which resulted in the formation of two new, transient peaks in our chromatogram that were identified to be the acyl phosphate ( $C_8-C_6P$ ) and the symmetric anhydride ( $C_8C_8$ , see Supplementary Figure S1). The  $C_8C_8$  was shortlived and fully decayed with 2.5 hours. Instead, the  $C_8-C_6P$  decayed over four days. Between 1 and 2.5 hours, the EDC was consumed while  $C_8C_8$  was still present. In that short time

window, C<sub>8</sub>-C<sub>6</sub>P increased, from which we conclude that part of the C<sub>8</sub>-C<sub>6</sub>P is synthesized through the C<sub>8</sub>C<sub>8</sub> intermediate (black arrow in Figure 1A), which is in line with very recent work by von Delius and coworkers.<sup>35</sup> Additionally, we observed a decrease in the concentration for both C<sub>8</sub>. We detected the micromolar concentrations of by-product N-acyl urea (Supplementary Figure S4). We could only detect C<sub>6</sub>P by LCMS but not HPLC due to the UV-transparency of alkyl phosphates. We further confirmed the absence of detectable amounts of by-products that could be produced by EDC and alkyl phosphates, *e.g.*, dialkyl pyrophosphate or the P-N adduct of the phosphate and EDU. We used the HPLC data to write a kinetic model that predicts the concentration of all species involved in the chemical reaction cycle (See methods section in the Supplementary Information). The model solves a set of ordinary differential equations and fits it to the experimental data, minimizing an error function using a least mean square method. We validated the kinetic constants we obtained from fitting one set of typical reaction conditions by predicting the kinetic profiles of all compounds involved at different fuel levels and starting acid/phosphate concentrations. The set of rate constants reasonably fitted the experimentally measured kinetic profiles at varying fuel and starting acid/phosphate concentrations well (See Supporting Table S1). The C<sub>8</sub>-C<sub>8</sub> symmetric anhydride then rapidly reacts further to form the C<sub>8</sub>-C<sub>6</sub>P. The model further predicts that the half-life of C<sub>8</sub>-C<sub>6</sub>P to be  $t_{1/2} = 16$  hours.

To study the formation of vesicles, the same reaction (40 mM C<sub>8</sub>, 40 mM C<sub>6</sub>P, 20 mM EDC) as above was performed in the presence of merocyanine 540—a dye used for quantifying lipid domains.<sup>36-39</sup> We found that the intensity of the MC540 increased drastically in the first tens of minutes after adding fuel to the reaction solution (Figure 1C). It peaked at around two hours, after which it steadily declined and reached its original value after over two days. Adding less fuel, *e.g.*, 15, 10, or 5 mM, shortened the reaction cycle and the maximum emission intensity of the dye. To ensure that the increased intensity originated from forming vesicles, we performed cryogenic transmission electron microscopy (cryo-TEM) imaging of the reaction mixture (Figure 1D). Excitingly, after 6 hours, we found multilamellar vesicles of irregular shape and polydisperse.

Next, we tested the critical fuel needed to initiate the vesicle formation. We used the MC450 assay four hours after the fuel addition as a proxy for vesicle formation (Figure 1D). For the reaction mixture with C<sub>6</sub>P and C<sub>8</sub>, we observed the first evidence of vesicles after adding a minimum of 4.5 mM of fuel. Using the kinetic model, we could calculate that the reaction cycle had produced a maximum of 1.7 mM of the acyl phosphate C<sub>8</sub>C<sub>6</sub>P. We thus considered the critical vesicle concentration CVC of C<sub>8</sub>C<sub>6</sub>P to be 1.7 mM. We performed the same experiment with 20 mM C<sub>8</sub>P and 20 mM C<sub>8</sub> and found that a minimum of 1.3 mM was required for the first indication of vesicles. According to the kinetic model, that corresponds

to a CVC for  $C_8C_8P$  of 0.35 mM. Noteworthy, the decrease of the CVC by roughly an order of magnitude follows the two-carbon rule for solubilities of aliphatic compounds. Finally, when  $C_6$  and  $C_6P$  were fueled with a maximum of 20 mM EDC, we could not observe any evidence of vesicle formation.

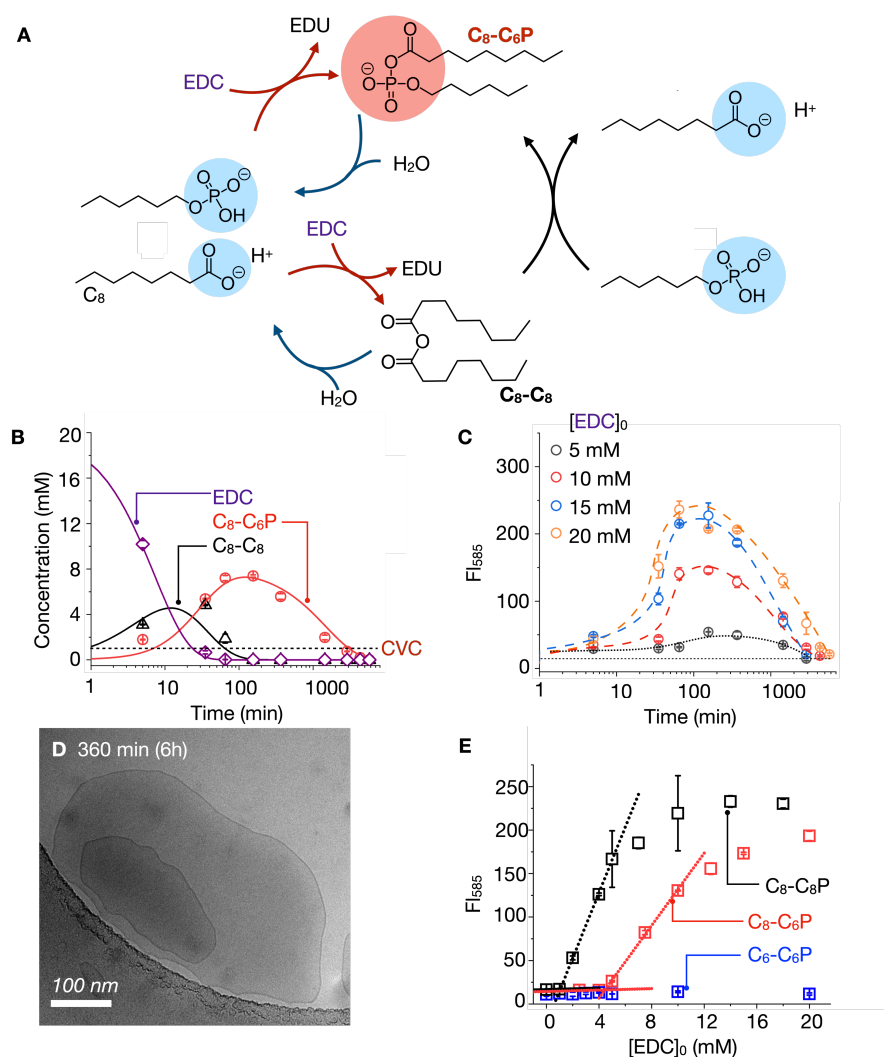


**Figure 1. Formation of dynamic, transient acyl phosphate-based vesicles at the expense of activation agents.** **A.** The acyl phosphate-producing chemical reaction network. **B.** The concentrations of the components of the reaction cycle against time when 40 mM  $C_8$  and 40 mM  $C_6P$  were fueled with 20 mM EDC at pH 6 in 200 mM MES buffer with 100 mM pyridine. Markers represent the HPLC data; solid lines represent data calculated by the kinetic model. **C.** MC540 fluorescence intensity against time ( $\lambda_{max} = 585$  nm) with 5, 10, 15, and 20 mM under otherwise similar conditions as B. The lines are added to guide the eye. **D.** Representative cryo-TEM image under the same conditions as described in B after 6 hours. **E.** MC540 fluorescence intensity after 4 hours after adding different amounts of fuel. Experiments were performed with  $C_6$  mixed with 40 mM  $C_6P$  (blue), 40 mM  $C_8$  mixed with 40

*mM C<sub>6</sub>P (red), or 20 mM C<sub>8</sub> mixed with 20 mM C<sub>8</sub>P (black) in 200 mM MES buffer with 100 mM pyridine.*

We further investigated the nature of vesicles by confocal fluorescence microscopy. We used the reaction mixture of 40 mM C<sub>8</sub> with 40 mM C<sub>6</sub>P and 20 mM EDC in the presence of MC540. We obtained confocal micrographs of the reaction mixture at various time points (Figure 2A, Supplementary Figure S5-S8). After 30 minutes, we found the first evidence of assemblies that were too tiny to resolve—they were either oil droplets or vesicles. Given that MC540 is hydrophilic and preferentially stains bilayers, we assume they were small vesicles, which also aligns with our finding by Cryo-TEM. After 9 hours, the vesicles had grown to multiple micrometers in diameter, and their membranes could easily be resolved. After 15 hours, as the vesicles were decaying, we observed that they underwent a morphological transition, *i.e.*, only a few large vesicles were found, and most had merged with a large, spherical assembly that had incorporated a large amount of MC540, given their high fluorescence intensity. After 24 hours, no vesicles were detected in the reaction mixture; instead, there were just bright micrometer-sized spherical assemblies. We hypothesize that the spherical assembly is a sponge-like, continuous lipid phase given that it had incorporated MC540 than a typical bilayer. Moreover, cryo-TEM after 24 hours revealed the formation of a spongelike phase with interlamellar attachment points (See Supplementary Figure S9). After 48 hours, the sample was mostly free of any assemblies corroborating the transient nature of the vesicles. To better understand the nature of the vesicles, we isolated them from their surrounding solution by spinning them down in a centrifuge after 6, 15, and 24 hours. The pellet was resuspended in buffer and analyzed by HPLC for its composition. Early in the cycle, *i.e.*, after 6 or 15 hours, the vesicles comprised almost equal parts of the C<sub>6</sub>P, C<sub>8</sub>, and C<sub>8</sub>C<sub>6</sub>P. Later in the cycle, we found that the fraction of C<sub>6</sub>P had increased at the cost of both C<sub>8</sub> and C<sub>8</sub>C<sub>6</sub>P. Noteworthy, the reaction cycle with C<sub>8</sub> and C<sub>8</sub>P also produced vesicles as evidenced by confocal and electron microscopy (See Supplementary Figure S10).

From the data above, we establish a tentative model to describe the self-assembly process of the components in the reaction cycle in response to chemical fuel (Figure 2C). First, the self-assembly can only occur in response to fuel, from which we conclude that the bilayer formation is driven by the formation of the acyl phosphate C<sub>8</sub>C<sub>6</sub>P. Nevertheless, the assembly is a coassembly of C<sub>6</sub>P, C<sub>8</sub>, and C<sub>8</sub>C<sub>6</sub>P, as evidenced by the spin-down experiments. We hypothesize that all components co-assemble to form a bilayer with the aliphatic tails pointing inward. As the system runs out of chemical fuel, no new C<sub>8</sub>C<sub>6</sub>P is formed. Thus, with time, the C<sub>8</sub>C<sub>6</sub>P concentration decreases, which also changes the ratio of the components in the assembly—more C<sub>6</sub>P and C<sub>8</sub> accumulate in the assemblies. That



shift in the ratio drives a change in the packing of the bilayer such that a bicontinuous bilayer phase that comprises mostly C<sub>6</sub>P forms. Finally, when all C<sub>8</sub>C<sub>6</sub>P is hydrolyzed, the bicontinuous bilayer phase dissolves, and the system is reset.

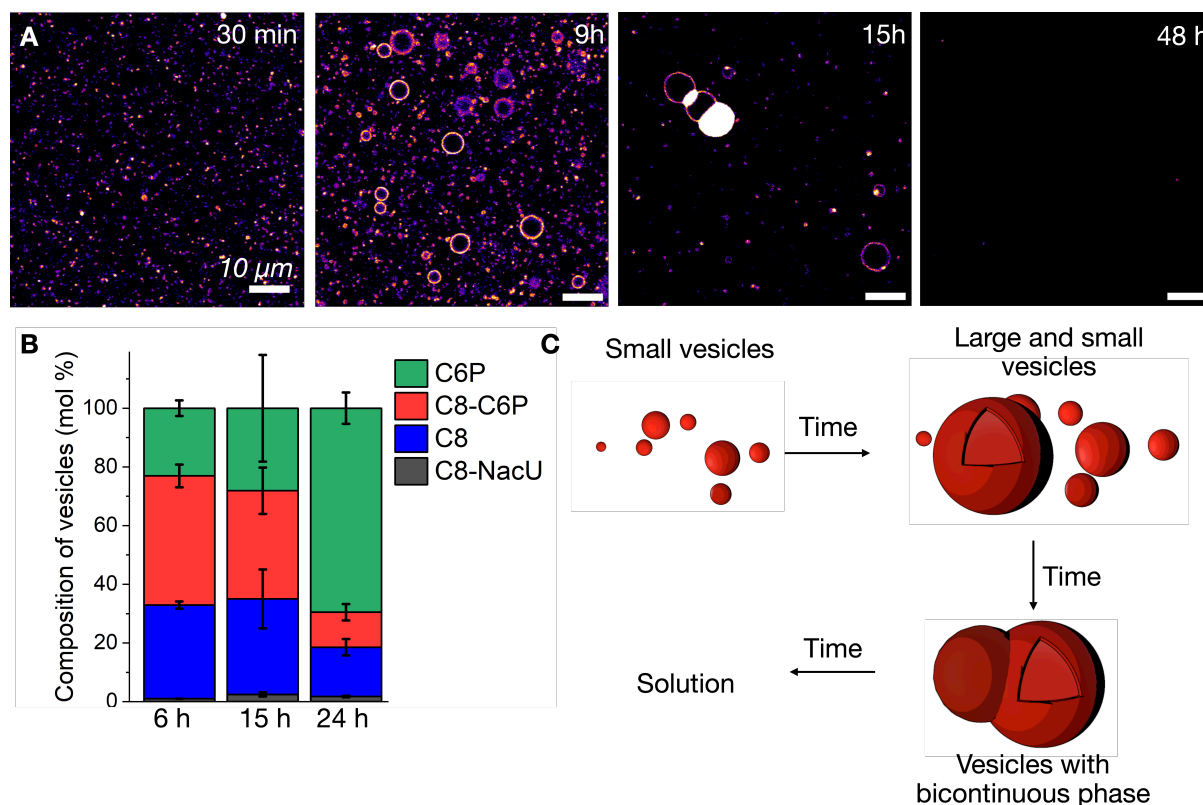


**Figure 2.** **A.** Confocal micrographs of 40 mM C<sub>8</sub> and 40 mM C<sub>6</sub>P fueled with 20 mM EDC in 200 mM MES pH 6 and 100 mM pyridine. Various time points demonstrate the formation of the vesicles and their transition to the bicontinuous phase in the later stages of the reaction cycle with subsequent decay. **B.** The composition of the vesicles at various time points of the reaction cycle. **C.** Schematic representation of the emergence and morphological transition of the vesicles during the reaction cycle.

Next, we tested whether the self-sustaining vesicles from simple building blocks could also be formed using prebiotically plausible fuels. Instead of EDC, we thus used the condensing agents 2-cyanoguanidine, cyanamide, dicyandiamide, and methyl isocyanide (Figure 3A), all of which have been proposed to be present on early earth before the emergence of life.<sup>40-41</sup> We used 100 mM of each condensing agent to fuel the reaction networks of 40 mM of C<sub>8</sub> and C<sub>6</sub>P. Unlike the previous experiments, we did not use MES as a buffer but only used pyridine. For 2-cyanoguanidine and cyanamide, we found no evidence of the acyl phosphate by HPLC-MS. For dicyandiamide, we found only traces of the acyl phosphate in the mass spectrometer. Excitingly, for methyl isocyanide, we observed up to 4 mM of the acyl

phosphate  $C_8C_6P$ . Like the experiments above, we followed the evolution of the reaction cycle by HPLC MS (Figure 3B and Supplementary Figure 10). The concentration of  $C_8C_6P$  increased and peaked at around 24 hours, *i.e.*, later than when we used EDC as fuel. After that, the  $C_8C_6P$  concentration decayed steadily over the next few days. We refitted the HPLC data using the kinetic model. The kinetic model verified that the activation was slower with methyl isocyanide as fuel compared to EDC. Finally, we confirmed that the pH did not change throughout the experiment despite lacking a buffer (See Supplementary Figure 12). Next, we used the MC540 assay to verify that the system could produce self-sustaining vesicles using MIC as a fuel. We measured the intensity of the MC540 emission 24 hours after adding different amounts of fuel and determined that a minimum of 30 mM of MIC was needed to induce vesicle formation. Using the kinetic model, we calculated that this corresponded to a critical vesicle concentration of 1.1 mM  $C_8C_6P$ , which aligns with the CVC found for EDC as fuel. Finally, we imaged the solutions formed with 100 MIC using confocal microscopy. In line with using EDC as fuel, we found the emergence of small vesicles, which, throughout tens of hours, grew to large unilamellar vesicles. Again, towards the end of the cycle, the vesicles transitioned into vesicles with a bicontinuous phase.

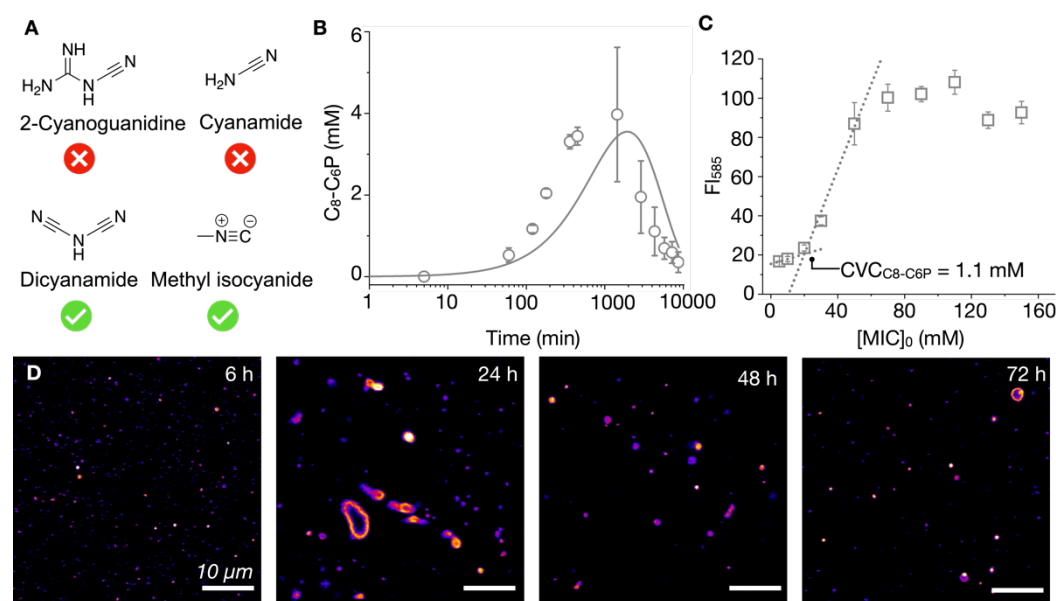


**Figure 3. Self-sustaining vesicles by prebiotic fuels.** **A.** Different prebiotically relevant fuels were tested in the acyl phosphate-producing reaction cycle. **B.** The concentration of  $C_8-C_6P$  against time when 40 mM  $C_8$  and 40 mM  $C_6P$  were fueled with 100 mM MIC. The solid line represents the data predicted by a kinetic model. **C.** The MC540 fluorescence intensity was measured 24 hours after adding different amounts of MIC to a solution as described in B. **D.** Confocal micrograph of the solution described in B at various time points.

## Conclusions



We presented a chemical reaction network that produces self-sustaining, dynamic vesicles based on simple molecules and driven by the conversion of activating agents. The reagents used in the network have been demonstrated to be prebiotically plausible, and the fuel-dependent vesicle could thus be used as a protocell model. In future work, we will combine these self-sustaining vesicles with catalysts, for example, catalysts that can convert prebiotic reagents into condensing agents driven by light. We will also combine the protocells with RNA sequences to test whether a pre-genotype, in the form of information containing RNA, can influence the behavior of the protocells, for example, their ability to survive starvation periods or their ability to divide.

## Acknowledgments

The BoekhovenLab is grateful for support from the TUM Innovation Network - RISE funded through the Excellence Strategy and the European Research Council (ERC starting grant 852187). This research was conducted within the Max Planck School Matter to Life, supported by the German Federal Ministry of Education and Research (BMBF) in collaboration with the Max Planck Society. This research was supported by the Excellence Cluster ORIGINS, which is funded by the Deutsche Forschungsgemeinschaft (DFG, German Research Foundation) under Germany's Excellence Strategy – EXC-2094 – 390783311. Cryo-TEM measurements were performed using infrastructure contributed by the Dietz Lab and the TUM EM Core Facility. We acknowledge the technical support provided by Fabian Kohler.

**Keywords:** chemically fueled self-assembly; self-sustaining compartments; protocells; fuel-driven

## References

1. Wang, X.; Du, H.; Wang, Z.; Mu, W.; Han, X., Versatile Phospholipid Assemblies for Functional Synthetic Cells and Artificial Tissues. *Adv. Mater.* **2021**, *33* (6), 2002635.
2. Lu, Y.; Allegri, G.; Huskens, J., Vesicle-based artificial cells: materials, construction methods and applications. *Materials Horizons* **2022**, *9* (3), 892-907.
3. Hanczyc, M. M.; Fujikawa, S. M.; Szostak, J. W., Experimental models of primitive cellular compartments: encapsulation, growth, and division. *Science* **2003**, *302* (5645), 618-622.
4. Chen, I. A.; Roberts, R. W.; Szostak, J. W., The Emergence of Competition Between Model Protocells. *Science* **2004**, *305* (5689), 1474-1476.
5. Zhu, T. F.; Szostak, J. W., Coupled Growth and Division of Model Protocell Membranes. *J. Am. Chem. Soc.* **2009**, *131* (15), 5705-5713.
6. Hentrich, C.; Szostak, J. W., Controlled Growth of Filamentous Fatty Acid Vesicles under Flow. *Langmuir* **2014**, *30* (49), 14916-14925.
7. Hanczyc, M. M.; Szostak, J. W., Replicating vesicles as models of primitive cell growth and division. *Curr. Opin. Chem. Biol.* **2004**, *8* (6), 660-664.

8. Todd, Z. R.; Cohen, Z. R.; Catling, D. C.; Keller, S. L.; Black, R. A., Growth of prebiotically plausible fatty acid vesicles proceeds in the presence of prebiotic amino acids, dipeptides, sugars, and nucleic acid components. *Langmuir* **2022**, *38* (49), 15106-15112.
9. Donau, C.; Boekhoven, J., The chemistry of chemically fueled droplets. *Trends in Chemistry* **2023**.
10. Donau, C.; Späth, F.; Stasi, M.; Bergmann, A. M.; Boekhoven, J., Phase Transitions in Chemically Fueled, Multiphase Complex Coacervate Droplets. *Angew. Chem. Int. Ed.* **2022**, *61* (46), e202211905.
11. Wanzke, C.; Jussupow, A.; Kohler, F.; Dietz, H.; Kaila, V. R. I.; Boekhoven, J., Dynamic Vesicles Formed By Dissipative Self-Assembly. *ChemSystemsChem* **2020**, *2* (1), e1900044.
12. Chen, X.; Würbser, M. A.; Boekhoven, J., Chemically Fueled Supramolecular Materials. *Accounts of Materials Research* **2023**, *4* (5), 416-426.
13. Schwarz, P. S.; Tena-Solsona, M.; Dai, K.; Boekhoven, J., Carbodiimide-fueled catalytic reaction cycles to regulate supramolecular processes. *Chem. Commun.* **2022**, *58* (9), 1284-1297.
14. Rieß, B.; Grötsch, R. K.; Boekhoven, J., The design of dissipative molecular assemblies driven by chemical reaction cycles. *Chem* **2020**, *6* (3), 552-578.
15. Boekhoven, J.; Hendriksen, W. E.; Koper, G. J. M.; Eelkema, R.; van Esch, J. H., Transient assembly of active materials fueled by a chemical reaction. *Science* **2015**, *349* (6252), 1075-1079.
16. van Ravensteijn, B. G. P.; Hendriksen, W. E.; Eelkema, R.; van Esch, J. H.; Kegel, W. K., Fuel-Mediated Transient Clustering of Colloidal Building Blocks. *J. Am. Chem. Soc.* **2017**, *139* (29), 9763-9766.
17. Kariyawasam, L. S.; Hartley, C. S., Dissipative Assembly of Aqueous Carboxylic Acid Anhydrides Fueled by Carbodiimides. *J. Am. Chem. Soc.* **2017**, *139* (34), 11949-11955.
18. Hossain, M. M.; Atkinson, J. L.; Hartley, C. S., Dissipative Assembly of Macrocycles Comprising Multiple Transient Bonds. *Angew. Chem. Int. Ed.* **2020**, *59* (33), 13807-13813.
19. Tena-Solsona, M.; Rieß, B.; Grötsch, R. K.; Löhner, F. C.; Wanzke, C.; Käsdorf, B.; Bausch, A. R.; Müller-Buschbaum, P.; Lieleg, O.; Boekhoven, J., Non-equilibrium dissipative supramolecular materials with a tunable lifetime. *Nature communications* **2017**, *8* (1), 15895.
20. Tena-Solsona, M.; Wanzke, C.; Riess, B.; Bausch, A. R.; Boekhoven, J., Self-selection of dissipative assemblies driven by primitive chemical reaction networks. *Nature Communications* **2018**, *9* (1), 2044.
21. Borsley, S.; Kreidt, E.; Leigh, D. A.; Roberts, B. M. W., Autonomous fuelled directional rotation about a covalent single bond. *Nature* **2022**, *604* (7904), 80-85.
22. Afrose, S. P.; Bal, S.; Chatterjee, A.; Das, K.; Das, D., Designed negative feedback from transiently formed catalytic nanostructures. *Angew. Chem.* **2019**, *131* (44), 15930-15934.
23. van der Helm, M. P.; Wang, C.-L.; Fan, B.; Macchione, M.; Mendes, E.; Eelkema, R., Organocatalytic Control over a Fuel-Driven Transient-Esterification Network\*\*. *Angew. Chem. Int. Ed.* **2020**, *59* (46), 20604-20611.
24. Maiti, S.; Fortunati, I.; Ferrante, C.; Scrimin, P.; Prins, L. J., Dissipative self-assembly of vesicular nanoreactors. *Nature Chemistry* **2016**, *8* (7), 725-731.
25. Sorrenti, A.; Leira-Iglesias, J.; Sato, A.; Hermans, T. M., Non-equilibrium steady states in supramolecular polymerization. *Nature Communications* **2017**, *8* (1), 15899.
26. Chen, C.; Valera, J. S.; Adachi, T. B. M.; Hermans, T. M., Efficient Photoredox Cycles to Control Perylenediimide Self-Assembly\*\*. *Chemistry – A European Journal* **2023**, *29* (1), e202202849.
27. Sharko, A.; Spitzbarth, B.; Hermans, T. M.; Eelkema, R., Redox-Controlled Shunts in a Synthetic Chemical Reaction Cycle. *J. Am. Chem. Soc.* **2023**, *145* (17), 9672-9678.
28. Del Grosso, E.; Prins, L. J.; Ricci, F., Transient DNA-Based Nanostructures Controlled by Redox Inputs. *Angew. Chem. Int. Ed.* **2020**, *59* (32), 13238-13245.

29. Zwicker, D.; Seyboldt, R.; Weber, C. A.; Hyman, A. A.; Jülicher, F., Growth and division of active droplets provides a model for protocells. *Nature Physics* **2017**, *13* (4), 408-413.
30. Nakashima, K. K.; van Haren, M. H. I.; André, A. A. M.; Robu, I.; Spruijt, E., Active coacervate droplets are protocells that grow and resist Ostwald ripening. *Nature Communications* **2021**, *12* (1), 3819.
31. Donau, C.; Späth, F.; Sosson, M.; Kriebisch, B. A. K.; Schnitter, F.; Tena-Solsona, M.; Kang, H.-S.; Salibi, E.; Sattler, M.; Mutschler, H.; Boekhoven, J., Active coacervate droplets as a model for membraneless organelles and protocells. *Nature Communications* **2020**, *11* (1), 5167.
32. Bonfio, C.; Caumes, C. c.; Duffy, C. D.; Patel, B. H.; Percivalle, C.; Tsanakopoulou, M.; Sutherland, J. D., Length-selective synthesis of acylglycerol-phosphates through energy-dissipative cycling. *J. Am. Chem. Soc.* **2019**, *141* (9), 3934-3939.
33. Chen, X.; Soria-Carrera, H.; Zozulia, O.; Boekhoven, J., Suppressing catalyst poisoning in the carbodiimide-fueled reaction cycle. *Chemical Science* **2023**, *14* (44), 12653-12660.
34. Chen, X.; Stasi, M.; Rodon-Fores, J.; Großmann, P. F.; Bergmann, A. M.; Dai, K.; Tena-Solsona, M.; Rieger, B.; Boekhoven, J., A Carbodiimide-Fueled Reaction Cycle That Forms Transient 5(4H)-Oxazolones. *J. Am. Chem. Soc.* **2023**, *145* (12), 6880-6887.
35. Englert, A.; Majer, F.; Schiessl, J.; Kuehne, A.; von Delius, M., Acylphosphates as versatile transient species in reaction networks and optical catalyst screenings. **2023**.
36. Williamson, P.; Mattocks, K.; Schlegel, R. A., Merocyanine 540, a fluorescent probe sensitive to lipid packing. *Biochimica et Biophysica Acta (BBA)-Biomembranes* **1983**, *732* (2), 387-393.
37. Langner, M.; Hui, S. W., Merocyanine 540 as a fluorescence indicator for molecular packing stress at the onset of lamellar-hexagonal transition of phosphatidylethanolamine bilayers. *Biochimica et Biophysica Acta (BBA) - Biomembranes* **1999**, *1415* (2), 323-330.
38. Watala, C.; Waczulikova, I.; Wieclawska, B.; Rozalski, M.; Gresner, P.; Gwoździński, K.; Mateasik, A.; Šikurova, L., Merocyanine 540 as a fluorescent probe of altered membrane phospholipid asymmetry in activated whole blood platelets. *Cytometry* **2002**, *49* (3), 119-133.
39. Dutta, R.; Pyne, A.; Kundu, S.; Banerjee, P.; Sarkar, N., Concentration-Driven Fascinating Vesicle-Fibril Transition Employing Merocyanine 540 and 1-Octyl-3-methylimidazolium Chloride. *Langmuir* **2017**, *33* (38), 9811-9821.
40. Nichols, C. M.; Wang, Z.-C.; Yang, Z.; Lineberger, W. C.; Bierbaum, V. M., Experimental and Theoretical Studies of the Reactivity and Thermochemistry of Dicyanamide: N(CN)<sub>2</sub><sup>-</sup>. *The Journal of Physical Chemistry A* **2016**, *120* (7), 992-999.
41. Remijan, A. J.; Hollis, J. M.; Lovas, F. J.; Plusquellic, D. F.; Jewell, P., Interstellar isomers: The importance of bonding energy differences. *The Astrophysical Journal* **2005**, *632* (1), 333.
42. Ibba, M.; Söll, D., Aminoacyl-tRNA synthesis. *Annu. Rev. Biochem* **2000**, *69* (1), 617-650.
43. Schoffstall, A. M., Prebiotic phosphorylation of nucleosides in formamide. *Origins of life* **1976**, *7* (4), 399-412.
44. Biron, J.-P.; Pascal, R., Amino Acid N-Carboxyanhydrides: Activated Peptide Monomers Behaving as Phosphate-Activating Agents in Aqueous Solution. *J. Am. Chem. Soc.* **2004**, *126* (30), 9198-9199.
45. Dai, K.; Pol, M. D.; Saile, L.; Sharma, A.; Liu, B.; Thomann, R.; Trefs, J. L.; Qiu, D.; Moser, S.; Wiesler, S., Spontaneous and Selective Peptide Elongation in Water Driven by Aminoacyl Phosphate Esters and Phase Changes. *J. Am. Chem. Soc.* **2023**.
46. Whicher, A.; Camprubi, E.; Pinna, S.; Herschy, B.; Lane, N., Acetyl phosphate as a primordial energy currency at the origin of life. *Origins of Life and Evolution of Biospheres* **2018**, *48*, 159-179.

47. Liu, Z.; Wu, L.-F.; Xu, J.; Bonfio, C.; Russell, D. A.; Sutherland, J. D., Harnessing chemical energy for the activation and joining of prebiotic building blocks. *Nature Chemistry* **2020**, *12* (11), 1023-1028.
48. Bowler, F. R.; Chan, C. K. W.; Duffy, C. D.; Gerland, B.; Islam, S.; Powner, M. W.; Sutherland, J. D.; Xu, J., Prebiotically plausible oligoribonucleotide ligation facilitated by chemoselective acetylation. *Nature Chemistry* **2013**, *5* (5), 383-389.